Chemical Engineering Journal xxx (xxxx) xxx–xxx

Contents lists available at ScienceDirect

Chemical Engineering Journal

journal homepage: www.elsevier.com/locate/cej

A modeling study on reaction and diffusion in MTO process over SAPO-34 zeolites

Mingbin Gao[a,b], Hua Li[a], Miao Yang[a], Jibin Zhou[a,b], Xiaoshuai Yuan[a,b], Peng Tian[a], Mao Ye[a,*], Zhongmin Liu[a]

[a] Dalian National Laboratory for Clean Energy, National Engineering Laboratory for MTO, Dalian Institute of Chemical Physics, Chinese Academy of Sciences, Dalian 116023, China
[b] University of Chinese Academy of Sciences, Beijing 10049, China

HIGHLIGHTS

- A reaction-diffusion model based on the dual-cycle reaction mechanism and Maxwell-Stefan diffusion theory is developed.
- Effect of coke deposition on diffusion and adsorption isotherm is taken into account.
- The model is validated against experiments of MTO reaction over SAPO-34 zeolites with different crystal size.
- How diffusion affects catalyst lifetime and product selectivity in MTO reaction can be modeled.

ARTICLE INFO

Keywords:
MTO
Reaction-diffusion model
Dual-cycle mechanism
SAPO-34

ABSTRACT

In this work, a modeling approach based on the dual-cycle mechanism and Maxwell-Stefan diffusion theory is developed to investigate the reaction and diffusion in methanol-to-olefins (MTO) process over SAPO-34 zeolites. In this work, the effect of coke formation on diffusion and adsorption in SAPO-34 zeolites were taken into consideration. The diffusivities and adsorption isotherms of the molecules of reactant and main product were derived by experimental measurements of the uptake rate of guest molecules. This model was used to study MTO reaction over SAPO-34 zeolites with different crystal size. It is shown that the model can capture the main features of MTO reaction as obtained by experiments, for instance, the different roles of the olefins-base cycle and aromatic-base cycle at different stage of the reaction. This model can predict the evolution of activated coke and non-activated coke during the reaction process. In particular, the simulation results directly show that the formation of non-activated coke can cause the pore blocking inside SAPO-34 zeolites and constrain the diffusion of different guest molecules to various extend. This is essential for us to understand the effect diffusion on catalyst lifetime and product selectivity in MTO reaction over SAPO-34 zeolites.

1. Introduction

Methanol-to-olefins (MTO) has received considerable attention since 1970s due to its importance in the production of light olefins (mainly ethylene and propylene) from resources other than oil. Despite significant progress in fundamental research in the past decades [1], a recent milestone is that in 2010 the world's first commercial MTO unit was successfully commissioned in north China by the Dalian Institute of Chemical Physics [2,3]. By the end of 2017, twelve DMTO units have been put on steam with the total production capacity of 6.46 million ton per annum.

For MTO processes, SAPO-34 zeolites, which have CHA structure consisting of large cages with small 8-ring windows (ca. 3.8 Å), are considered as the most promising catalyst and the selectivity to the light olefins can exceed 80% [2]. The reaction mechanism of MTO over SAPO-34 zeolites is very involved. According to Dahl and Kolboe [4], a hydrocarbon pool (HCP) is formed in which the cyclic organic species (i.e. coke or aromatic compounds) confined inside the cages of SAPO-34 zeolites act as co-catalysts for the further assembly of olefins from methanol. Recent studies suggest that the formation of light olefins in MTO process follows the more complicated dual-cycle (i.e. an olefins-based cycle and aromatics-based cycle) reaction mechanism [1,5], as shown in Fig. 1(A). Both cycles are interdependent in MTO reaction [6,7]: the aromatic species generated by aromatization via the olefins-

* Corresponding author.
E-mail address: maoye@dicp.ac.cn (M. Ye).

https://doi.org/10.1016/j.cej.2018.08.054
Received 11 June 2018; Received in revised form 31 July 2018; Accepted 8 August 2018
1385-8947/

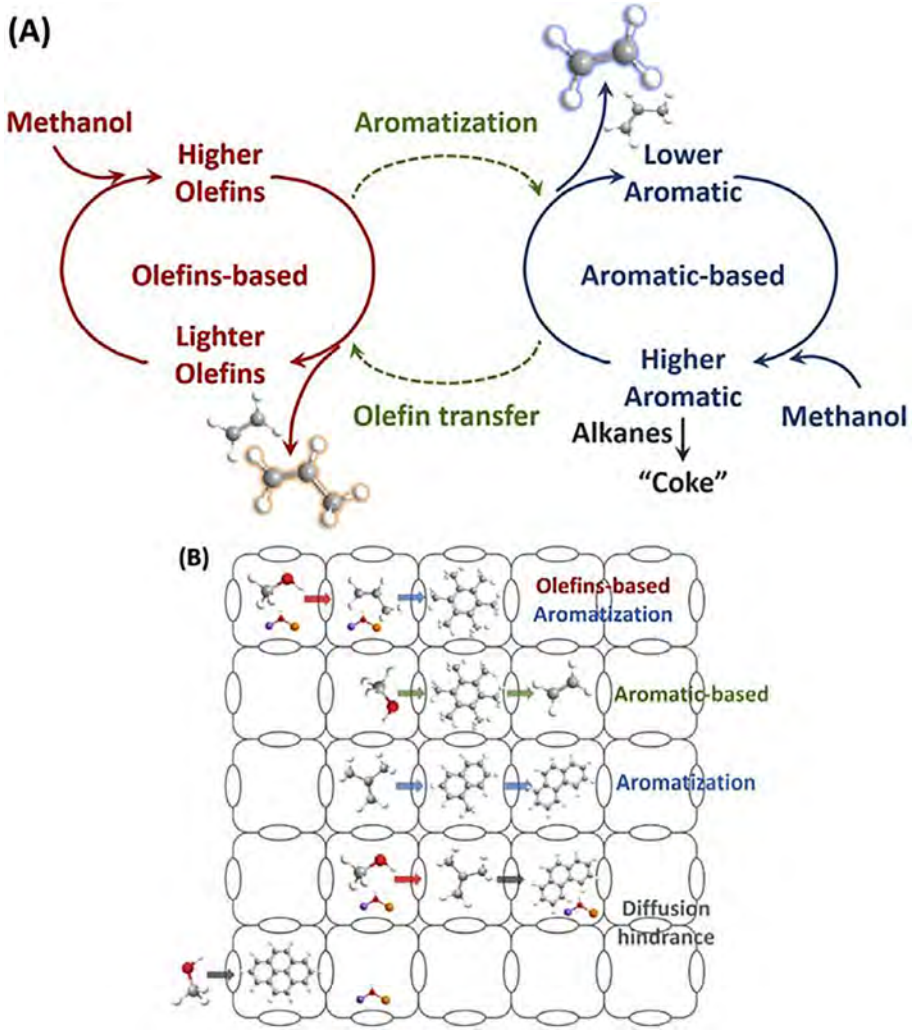

Fig. 1. (A) The scheme of dual-cycle mechanism in MTO reaction [7]; (B) the reaction and diffusion of reactant and product molecules in MTO reaction over SAPO-34 zeolites.

based cycle provide new active centers for the aromatic-based cycle, and the low-cyclic aromatics further evolve to the poly-cyclic aromatic compounds [8,9].

The poly-cyclic aromatics are considered as the main compounds of coke in MTO process, and the formation of which can first lead to a higher selectivity to light olefins and then cause rapid deactivation of catalyst [10–12]. The deposition of coke inside cages not only results in acid sites coverage [10,11], but also influences the diffusion of reactant and products [5,13,14]. Dai et al. [10] found that for increasing quantity of coke of SAPO-34 zeolites, the diffusion of the smaller size of olefins enhances in comparison to that of the larger size of alkanes. In the case of excess free acid sites, it has been anticipated that the diffusion restriction of poly-cyclic aromatics and branched hydrocarbons by the small 8-ring windows in SAPO-34 zeolites can prompt the selectivity to light olefins. It has been found that catalyst lifetime can be extended by reducing the crystal size of SAPO-34 zeolites [5,11,14–19].This is normally explained as the smaller crystal size has shorter diffusion path [5,19] and thus shorter residence time for reactant and product molecules, which could restrain the formation of poly-cyclic aromatic compounds and thus prolong the lifetime of SAPO-34 zeolites in MTO reaction. It is speculated that small SAPO-34 crystal size can slow down the formation rate of coke compounds [5,14,19], and lead to an increasing quantity of coke, especially the poly-cyclic aromatic compounds, inside cages after complete deactivation [5,14,19]. Cai et al. [20] showed that the formation of poly-cyclic aromatics may cause serve blocking of the pores and strong hinderance of the diffusion of reactant and product molecules inside SAPO-34 zeolites, which lead to the increase of inaccessible active sites and species for reactant and eventually the deactivation of catalyst.

The role of coke in SAPO-34 zeolites in MTO reaction has long been recognized, and as discussed above, the diffusion of reactant and product molecules inside SAPO-34 zeolites is of critical importance in understanding MTO reaction particularly in terms of catalyst lifetime and shift of product selectivity. A kinetic model capable of describing the reaction and diffusion in MTO process, therefore, is highly desired due to its significance in reactor design and operation optimization. MTO kinetic models developed so far mainly include lumped models [21–26] and microkinetics models [27–31]. In these developed models, coke formation (or catalyst deactivation) was normally considered by use of an empirical expression including exponential [29] and hyperbolic functions [21], in which the parameters were derived simply by fitting the experimental data. The empirical expression of catalyst deactivation cannot reveal the effect of diffusion on catalyst lifetime and the shift of product selectivity [5,11,13,19], and the effect of coke formation on diffusion of reactant and product molecules. To fill this gap, therefore, it is the goal of current work to establish a modeling approach that can account for the reaction and diffusion in MTO process over SAPO-34 zeolites.

In a catalyst pellet, different pore size implies different diffusion mechanism. For micropore (smaller than 2 nm), surface diffusion of

adsorbed molecular components along the pore wall surface is dominant. For macro/*meso*-pores, the bulk (or molecular) diffusion and Knudsen diffusion become important suppose that no strong adsorption exists. In addition, the pressure gradient inside the pellet cannot be neglected if there is a net change in the number of moles of guest molecules inside the porous catalyst, which can lead to the viscous or Darcy flow in the pellet [32–34]. In this work, the micropore SAPO-34 zeolite crystals is of interest, where the surface diffusion dominates. Theoretically, the adsorption isotherm and diffusion coefficient within micropore could be effectively predicted by means of molecular dynamics (MD) and Monte Carlo simulations [34–36]. However, the topology structure of zeolites used in the simulations normally has been greatly simplified, which will cause essential discrepancy between the predicted adsorption isotherm and diffusion coefficient and the real ones. Hence, in this work the surface diffusion coefficients were obtained from experimental measurement by uptake method, and the adsorption isotherms for multicomponent system by the ideal adsorbed solution theory (IAST) [37]. The Maxwell-Stefan model was used to obtain diffusion flux as it is more accurate than the Fickian diffusion approach for multicomponent system [38].

2. Modeling

2.1. Reaction and diffusion model

In the fixed bed reactor filled with zeolite catalysts, the reaction and mass transfer are formulated at two scales. At the single zeolite crystal scale, the reaction and diffusion processes (in particular the surface diffusion and MTO reaction) over SAPO-34 zeolites were considered. At the reactor scale, the advection in the axial direction and mass exchange between the gas flow and zeolite crystals were considered. The scheme of our modelling strategy is described in Fig. 2. As shown in Fig. 2, the fixed bed reactor is assumed to be composed of a number of perfectly mixed sub-reactors in series. In each sub-reactor, the zeolite crystals are assumed to be spherical and monodispersed.

At the single zeolite crystal scale, the change of loading of compound i with time due to reaction and diffusion is described by the following partial differential equations (PDEs) [39]:

$$\frac{\partial \rho_i}{\partial t} = -\nabla \cdot \vec{n}_i + R_i \tag{1}$$

where $\rho_i = M_i q_i \rho_{zeo.}$ represents the density of component i (kg·m^{-3}), M_i the molar mass of component i (kg·kmol^{-1}), q_i the loading of component i (kmol·kg$_{zeo.}^{-1}$), $\rho_{zeo.}$ the density of zeolite crystal (kg$_{zeo.}$·m^{-3}), t the time on stream (s), $\vec{n}_i = M_i \vec{N}_i$ the mass flux vector of compound i (kg·m^{-2}·s^{-1}), $\vec{N}_i$ the molar flux vector of compound i (kmol·m^{-2}·s^{-1}), and R_i the reaction rate of compound i (kg·m^{-3}·s^{-1}).

The molar flux vector $\vec{N}_i$ is predicted by the Maxwell-Stefan diffusion theory [32] via the n-compound equation [33,34]

$$-\frac{\theta_i}{RT}\nabla\mu_i = \sum_{\substack{j=1 \\ j\neq i}}^{n} \frac{q_j\vec{N}_i - q_i\vec{N}_j}{q_i^{sat} q_j^{sat} D_{ij}} + \frac{\vec{N}_i}{q_i^{sat} D_i} (i = 1, 2, \cdots, n) \tag{2}$$

where μ_i is the molar chemical potential of compound i (J·kmol^{-1}), R the gas constant (J·kmol^{-1}·K^{-1}), T the absolute temperature (K), q_i^{sat} the saturated adsorption capacity of compound i (kmol·kg$_{zeo.}^{-1}$), D_i the effectivity diffusion coefficient of compound i (m^2/s), D_{ij} the exchange coefficient between compound i and j (m^2/s), and θ_i the fractional occupancy of compound i which is defined as $\theta_i \equiv \frac{q_i}{q_i^{sat}}$ [32]. The gradient of chemical potential can be expressed in terms of the gradient in θ_i by introducing the thermodynamic correction factors Γ_{ij} [32],

$$-\frac{\theta_i}{RT}\nabla\mu_i = \sum_{j=1}^{n} \Gamma_{ij}\nabla\theta_j,\ \Gamma_{ij} = \frac{\theta_i}{p_i}\frac{\partial p_i}{\partial \theta_j} (i = 1, 2, \cdots, n) \tag{3}$$

Here p_i denotes the pressure of gas compound i (Pa), which can be related to θ_i via the measured adsorption isotherm. The solutions of Eqs. (2) and (3) for the fluxes can be given in the form of [32]

$$\begin{pmatrix} \vec{N}_1 \\ \vec{N}_2 \\ \vdots \\ \vec{N}_n \end{pmatrix} = -[B]^{-1}[\Gamma] \begin{pmatrix} \nabla q_1 \\ \nabla q_2 \\ \vdots \\ \nabla q_n \end{pmatrix} \tag{4}$$

with the elements of matrix $[B]$ are [32]

$$B_{ii} = \frac{1}{D_i} + \sum_{\substack{j=1 \\ j\neq i}}^{n} \frac{\theta_j}{D_{ij}},\ B_{ij(i\neq j)} = -\frac{q_i^{sat}}{q_j^{sat}}\frac{\theta_i}{D_{ij}} (i, j = 1, 2, \cdots, n) \tag{5}$$

The matrix of thermodynamic correction factors $[\Gamma]$ is calculated following the ideal adsorbed solution theory (IAST) [37] with the experimentally measured parameters of the pure-compound adsorption isotherm. It is reported that the adsorption isotherm of a pure-compound in SAPO-34 zeolite could be derived by the Langmuir adsorption model [40–42]

$$q_i = q_i^{sat}\frac{b_i p_i}{1 + b_i p_i} \tag{6}$$

where b_i is the Langmuir adsorption constant (Pa^{-1}).

The exchange coefficient D_{ij} is calculated via the interpolation of the

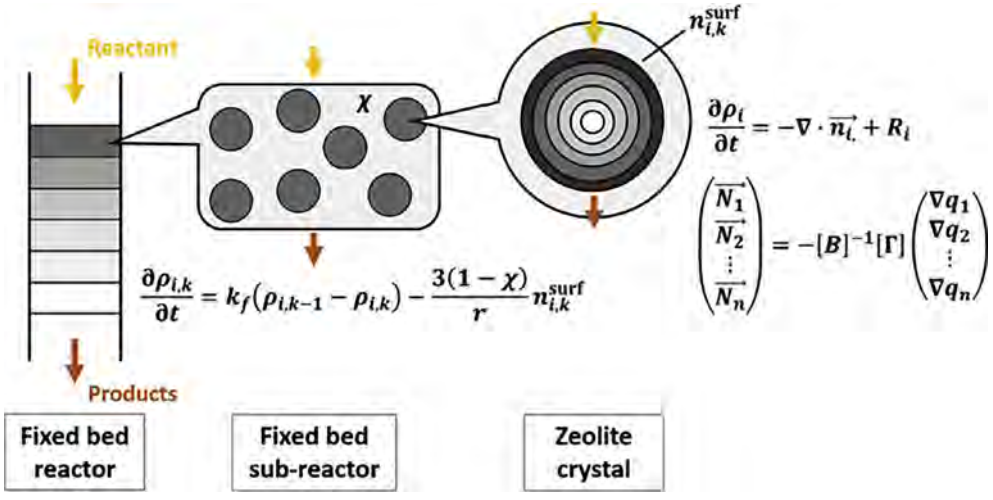

Fig. 2. The scheme of modelling strategy for reaction-diffusion process in the fixed bed reactor.

effective diffusion coefficients of pure-compound from experiment [33].

$$q_j^{\text{sat}} D_{ij} = q_i^{\text{sat}} D_{ji} = [q_j^{\text{sat}} D_i]^{\frac{q_i}{q_i+q_j}} [q_i^{\text{sat}} D_j]^{\frac{q_j}{q_i+q_j}} \tag{7}$$

At the fixed bed reactor scale, the governing equation for any given component in a sub-reactor could be written as

$$\chi \frac{\partial \rho_{i,k}}{\partial t} = k_f (\rho_{i,k-1} - \rho_{i,k}) + \frac{3(1-\chi)}{r} n_i^{\text{surf}} \tag{8}$$

where χ (dimensionless) is the voidage of catalyst bed, k_f the ratio of volume flow rate of feed to gas phase volume (s^{-1}), and $\rho_{i,k-1}$ the density of compound i in the $(k-1)$ th sub-reactor, r the effective radius of the zeolite crystal (m), and n_i^{surf} the net mass flux of compound i at boundary surface of zeolite crystal ($kg{\cdot}m^{-2}{\cdot}s^{-1}$). In this work, the density $\rho_{i,k-1}$ of the $(k-1)$ th sub-reactor is used as inlet density for calculating the density of the k th sub-reactor. The first term on the right side of the Eq. (8) represents the advection of gas flow in the reactor, and the second term represents the mass exchange between the gas flow and the zeolite crystals, and n_i^{surf} is in fact the magnitude of mass flux vector $\vec{n_i}$ at the surface of zeolite crystal. It should be stressed that the reaction term is not explicitly included in Eq. (8). Eq. (8) is indeed used for n species, with k_f is assumed to be constant.

Eq. (1) together with Eq. (8) can describe the reaction and diffusion processes in the fixed bed reactor. In this work, any single SAPO-34 zeolite crystal was assumed to be spherical and discretized in an annual mesh (mesh size of ca. 0.15 μm, as shown in Fig. 2) by use of the finite volume method (FVM). To optimize the number of ideal mixed sub-reactors to mimic the plug flow reactor, simulations by dividing the zeolite crystal bed into 2–4 sub-reactors were performed. As shown in Fig. S2 in Supporting information, the simulation results of methanol conversion and product selectivity only show minor difference. Thus, in the rest of this work it is assumed that the reactor is composed of two ideal mixed sub-reactors to mimic the plug flow reactor. The effect of coke formation on diffusion and adsorption isotherms is taken into consideration in our model, which will be further discussed in Section 4.3.

Note that Eqs. (1) and (8) are coupled by the diffusion flux n_i^{surf} at the boundary surface of zeolite crystal, and these equations were solved simultaneously. The time-dependent PDEs, describing the two scale processes, when discretized with respect to the spatial coordinate by use of FVM, can be reduced to time-dependent ordinary differential equations (ODEs). The reduced storage matrix method, which is the combination of Newton iteration, BDF methods, GMRES iteration and preconditioning for stiff reactions, was used to solve the stiff ODEs [33]. The time step of the ODEs is automatically controlled by presetting both the relative and absolute tolerance [43].

2.2. Reaction network

Recent studies found that the dual-cycle mechanism can better describe the MTO reaction [1,6,24], in which methanol conversion occurs simultaneously via an olefins-based and an aromatics-based cycle, as depicted in Fig. 1(A). Considering that the acid sites dominate the important reactions (i.e. protonation, methylation, alkylation and β-scission reaction) in the olefins-based cycle in methanol conversion [6,30], the amount of acid sites S is defined as a virtual lump which represents olefins-based cycle. In order to consider the effect of diffusion on the deactivation, the coke compounds are divided into activated coke A and non-activated coke N. From the experimental results [44] as well as DFT calculations [45], it is found that the monocyclic and bicyclic aromatics mainly serve as activated coke in MTO reaction, whereas tricyclic and polycyclic aromatics usually are considered as non-activated coke, which not only lower the reactivity but also hinder the diffusion of reactant and product molecules due to the pore blocking [5]. Thus the formation of aromatic compounds can be, as shown in Fig. 3, on the one hand equivalent to the change or coverage of the number of acid sites S [24,46], and on the other hand considered as consisting of the activated coke A and the non-activated coke N [45]. In the reaction network, the activated coke is mainly transformed from the olefin products in presence of acid sites, which can implicitly include the auto-catalytic process in MTO reaction. While the non-activated coke is formed via further aromatization of activated coke [6,46]. And the non-activated coke could promote the hydrogen transfer reaction of the reactant and product molecules to form alkanes, which is considered as the main reason for high selectivity to alkanes after catalyst deactivation [47]. The reaction network in this work was developed based on our recent work [24,48]. The major difference of the reaction network between this work and our previous work [48] is that the coke compounds R in previous were further divided into activated coke A and non-activated coke N in this work. In our previous work, the kinetic model was developed for catalyst pellet, which includes both zeolite crystals and binder (meso-/macropore). That is to say, such kinetic model represents the apparent kinetics accounting for the reaction inside the zeolite crystals and diffusion in both zeolite crystal and binder. In order to reflect the deactivation process of MTO reaction an empirical deactivation function had to be introduced in the kinetic model in our previous work, and the diffusion inside catalyst particle has not been explicitly considered. However, in this work, the diffusion is explicitly incorporated, and the deactivation of catalyst is a natural result of formation of non-activated coke. It should be noted that the parameters in our previous work cannot be directly used in this work because in the previous model the effect of diffusion was not decoupled. Therefore, in this work, all the kinetic parameters were fitted based on experimental data for SAPO-34 zeolites.

3. Experimental

3.1. Preparation and characterization of SAPO-34

SAPO-34 zeolites with different crystal size were synthesized, and the details of synthesis process can be found in [49]. These zeolites were characterized by field emission scanning electron microscope (FESEM), X-ray diffraction (XRD), NH_3-temperature programmed desorption (NH_3-TPD) and nitrogen adsorption and desorption isotherm, which are included in Supporting Information.

3.2. MTO reaction over SAPO-34 zeolites

The SAPO-34 zeolites were first calcinated at 600 °C for 6 h to remove organic template. After that the SAPO-34 zeolites powder was pressed into flakes at 20 MPa pressure, and then crushed into pellets and sieved to a diameter of 250–425 μm [25], which was loaded into the fixed bed reactor. No binder was used during pressing in order to avoid the introduction of meso/macropores into the catalyst, since only micropores are of interest in current work. The experiments of MTO reaction over different SAPO-34 zeolites were carried out in a quartz tubular fixed-bed reactor (inner diameter of 0.004 m, bed height of 0.010 m) at atmospheric pressure [24]. The reactor was first heated to 500 °C, maintained for 1 h while keeping the catalyst (100 mg) in nitrogen flow, and then adjusted to 450 °C. The liquid flow of methanol (99.5% purity) passed through a vaporizer before entering the reactor with nitrogen to guarantee well vaporization of liquid feed. The space velocity WHSV was set to 5.0 $g_{MeOH} \cdot g_{zeo.}^{-1} \cdot h^{-1}$ and partial pressure of methanol to 0.28 bar. Due to the small loading of catalyst and minor temperature difference at the axial direction, no inert material was added to dilute the catalyst in the fixed bed reactor. Knowing the zeolite density (1480 kg/m^3) [41], catalyst loading (100 mg), bed height and inner diameter of the reactor, we can estimate the voidage of the bed is around 0.5 in this work. On-line analysis of the gas products was performed with an Agilent 7890B gas chromatography equipped with a FID detector and a PoraPLOT Q-HT capillary column. The conversion

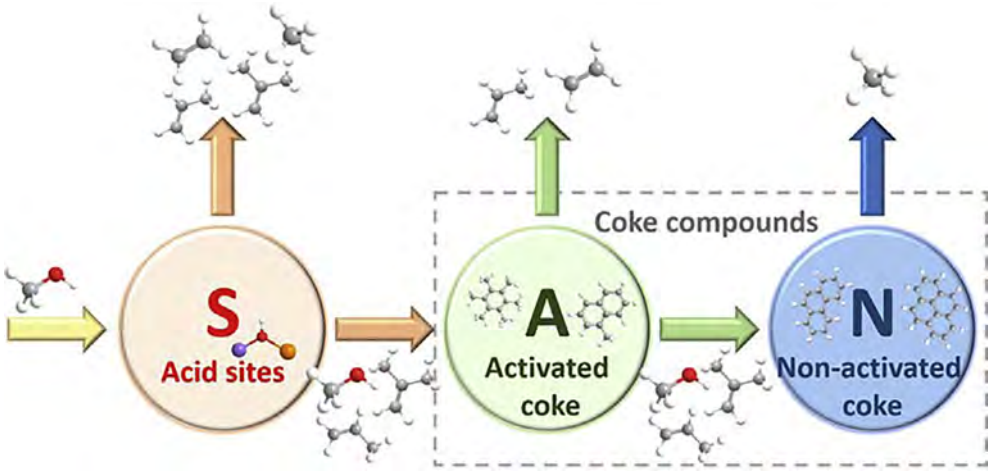

Fig. 3. The schematic of simplified reaction network for the MTO conversion.

and selectivity were calculated on CH_2 basis. Dimethyl ether (DME) was considered as reactant in the calculation. A set of experiments with same space velocity and partial pressure of methanol but different linear velocity and catalyst loading were also performed, and the results, as shown in Fig. S3 in Supporting Information, confirm that the effect of film diffusion can be ignored.

3.3. Analysis of coke species

The quantity of coke in SAPO-34 zeolites at different time on stream was determined by thermo-gravimetric analysis (TGA) on a SDT Q600 analyzer at the temperature range of 50–900 °C with a heating rate of 10 °C/min under an air flow of 100 mL/min. The retained coke in SAPO-34 zeolites at different time on stream were investigated by dissolution experiments according to the procedure introduced by Guisnet [50]. Typically, 25 mg of the spent SAPO-34 catalyst was dissolved in 1 mL HF solution (20 wt%) in a Teflon container. The confined aromatic compounds of the spent catalyst were extracted from the water phase by the addition of 1 mL CH_2Cl_2 containing C_2Cl_6 as internal standard. Analysis of the extracted phase was performed on an Agilent 7890A gas chromatography equipped with an Agilent 5795C mass selective detector with a HP-5 capillary column and a FID detector. The structure annotated onto the chromatograms are identified via peak identifications according to the NIST database.

Based on the FID signal of GC-MS chromatograms for hydrocarbon compounds, the weight percentage w_i of specific coke species in coke compounds can be first determined by use of the corresponding area A_i. Then the ratio of concentration between this specific coke species and internal standard (C_2Cl_6) could be obtained by modifying the standard curve (e.g. $c_i/c_{inter} = 0.1367*w_i/w_{inter} + 0.0078$ for methlbenzene). Note that the percentage of activated (or non-activated) coke is defined as the molar ratio of activated (or non-activated) coke to the total coke after complete deactivation. In this work, the concentration of internal standard is about 100 ppm (1 mL), the activated coke includes both monocyclic (average molar mass 113 g/mol) and bicyclic aromatics (average molar mass 130 g/mol), the non-activated coke lumps the tricyclic (average molar mass 185 g/mol) and other polycyclic (average molar mass 215 g/mol) aromatics [12]. After the quantities of main aromatic species are determined, the total quantity of activated (or non-activated) coke could be obtained subsequently.

3.4. Uptake rate and adsorption isotherm

The uptake rate and adsorption isotherm were measured by use of an Intelligent Gravimetric Analyzer (IGA-100, Hiden Analytical). Specially, to enhance permeability of probe gas or vapor in catalysts, mesh type sample cell was used. About 30 mg SAPO-34 zeolite was added to the chamber and outgassed until a constant weight is achieved at a pressure of 10^{-6} mbar and temperature of 350 °C for at least 6 h. Then flowrate of probe gas or vapor was adjusted carefully in order to maintain isobaric and isothermal conditions. Meanwhile, mass change (resolution of 0.1 μg) with buoyancy corrections, system pressure, and sample temperature were recorded in real-time. For entire adsorption process, the pressure of probe gas or vapor increased stepwise, and at each pressure an adsorption equilibrium was reached. All probe gas (i.e. ethylene of 99.995% purity, propylene of 99.99% purity, propane of 99.995% purity and *iso*-butylene of 99.5% purity) were purchased from Dalian Special Gases Co., Ltd. Methanol of 99.5% purity was purchased by Tianjin Kemiou Chemical Reagent Co., Ltd.

4. Results and discussion

4.1. Characterization of SAPO-34 zeolites

Fig. 4(A)–(C) shows the morphological pictures of SAPO-34 zeolites used in this work. The crystal size distributions of three SAPO-34 zeolite samples were measured by the images of FE-SEM, which are shown in Fig.S1 in Supporting Information, and average crystal size are respectively 8 μm for SAPO-L, 4 μm for SAPO-M and 1 μm for SAPO-S. Fig. 4(D) shows the XRD patterns, and as can be seen all samples exhibit typical patterns for the CHA topology with good crystalline purity. From the profile of NH_3-TPD in Fig. 4(E), the quantity of medium and strong acidity (about 450 °C) derived from the peak-differentiating analysis [51], is quite close for all three samples, which is in the range of 0.76–0.79 mmol/$g_{zeo.}$. Based on the nitrogen sorption isotherm shown in Fig. 4 (F), typical type I isotherms for microporous materials are observed for all three samples.

4.2. Catalytic performance of SAPO-34 zeolites

The results of methanol conversion and selectivity of the product molecules are shown in Fig. 5. For simplicity, we lumped the long-chain hydrocarbons as C_{4+} and the paraffin products including methane, ethane and propane as alkanes. At different time on steam, the SAPO-34 zeolites were discharged and the quantity of coke deposited on SAPO-34 zeolites as well as the retained aromatic compounds were analyzed, as shown in Fig. 6.

Fig. 5 shows the evolution of MTO reaction with time on stream, which can be divided into three stages: initial stage, steady reaction stage and deactivation stage. According to the dual-cycle mechanism, the lumped product C_{4+} is the precursor for the formation of low-cyclic aromatic compounds [46] at the initial stage. Notably, the selectivity to

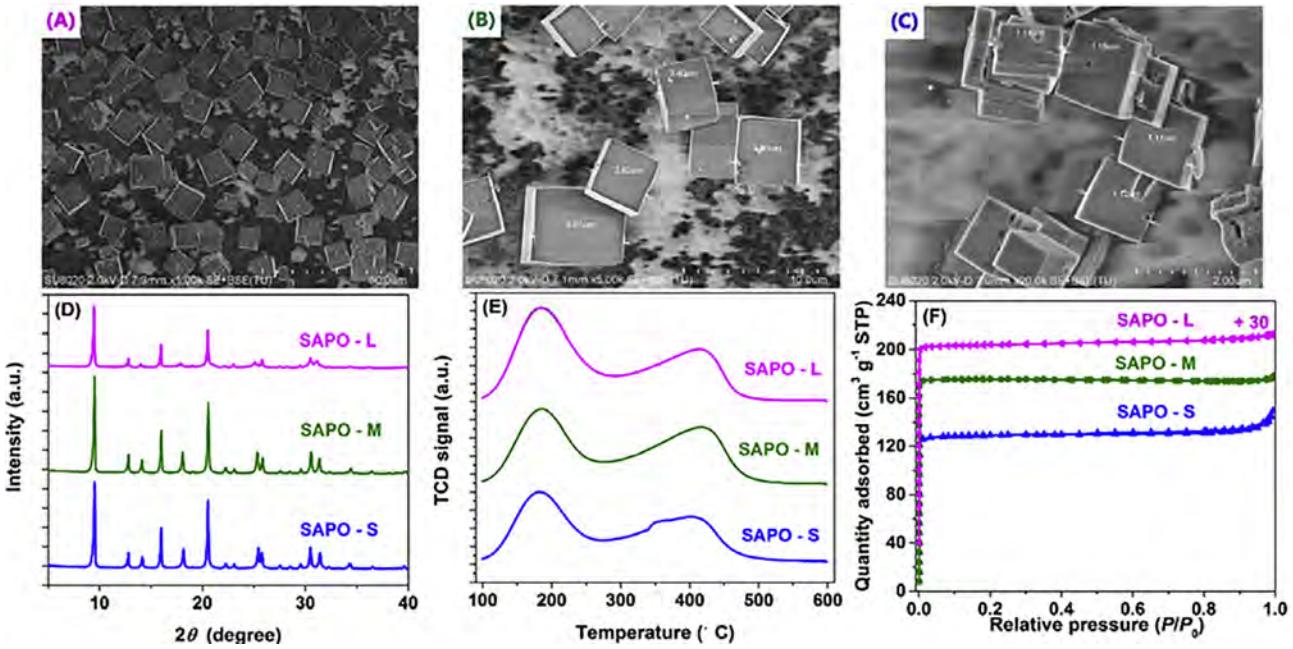

Fig. 4. Characterization results of SAPO-34 zeolites with different crystal size. (A)–(C) FESEM micrographs; (D) XRD patterns; (E) NH_3-TPD profiles; (F) nitrogen adsorption and desorption isotherms.

C_{4+} is relatively high for smaller crystal size, which demonstrates that decreasing crystal size could shorten the residence time of product molecules inside the zeolites. Meanwhile the formation of aromatic compounds was depressed due to the shorter diffusion pathway of product molecules, which is confirmed by the observation of the sluggish increase in the quantity of coke for the SAPO-34 zeolites with smaller crystal size as shown in Fig. 6. At the initial stage, the corresponding selectivity to ethylene for SAPO-34 zeolites with smaller crystal size is relatively lower, which could be deduced that the olefins-based cycle is the predominant mechanism at this stage. With methanol conversion proceeding, the selectivity to C_{4+} shows continuous declination (see Fig. 5) but the production of aromatic compounds steadily increases (as shown in Fig. 6), including both activated and non-activated coke. This indicates a shift of the predominant mechanism to aromatics-based cycle, and thus the selectivity to ethylene may also increases rapidly. At the steady stage, as shown in Fig. 6, a significant amount of activated coke was detected, and the activated coke constitutes the active HCP compounds in MTO process [1,2]. Therefore, at the steady stage the methanol conversion is still close to 100%. But a rapid decrease of the density of accessible Brønsted acid sites is expected, as evidenced by the experiments with ^{1}H MAS NMR [10,11]. When a dramatical decrease of methanol conversion is observed, it evolves into the deactivation stage. As can be seen from Figs. 5and 6, at this stage the selectivity to C_{4+} and the quantity of activated coke decline markedly, and the selectivity to methane and the amount of non-activated coke increase. This suggests that the diffusion of propylene and C_{4+} is significantly hindered due to the presence of non-activated coke [5], which significantly promotes the aromatization and hydrogen transfer of propylene, C_{4+} and activated coke due to the prolonged residence time of product molecules in SAPO-34 zeolites. The selectivity to ethylene is still increasing, which may be resulted from different diffusion hindrance for smaller molecules by non-activated coke [5], and this will be further discussed in Section 4.4. A comparison between the retained aromatic compounds in SAPO-34 zeolites of complete deactivation in the three catalysts reveals that the amount of coke and non-activated coke are higher for small crystal. This result may suggest that the active sites could be utilized more fully due to more shorter resistance time of reactant and product molecules in small crystal of SAPO-34.

4.3. Uptake rate and adsorption isotherm

To quantify to what extent the diffusion resistance is affected by guest molecules, the diffusivities of different molecules were measured by uptake rate method. Fig. 7(A) shows the experimental uptake rate for methanol, ethylene, propylene and *iso*-butylene in fresh SAPO-34 zeolites. To fit the experimental results, the effective diffusion coefficient was estimated using Fick's second law [52],

$$\frac{m(t)}{m(\infty)} = \frac{6}{\sqrt{\pi}}\sqrt{\frac{D}{r^2}}\sqrt{t} \tag{9}$$

where $m(t)/m(\infty)$ is the normalized loading and r the effective radius of the zeolite crystal (m) which is defined as the radius of a sphere with the same surface to volume ratio as the crystal. Fig. 7(A) shows there exists a linear relationship between $m(t)/m(\infty)$ and $t^{1/2}$, and the effective diffusion coefficients could be calculated from the slopes, which are summarized in Table 1. The results show that the effective diffusion coefficients increase in the following order: *iso*-butylene < propylene < methanol < ethylene < methane. Such an order can be directly related to the decrease in residence time of corresponding molecules in SAPO-34 zeolites. For the further verification, the measured effective diffusion coefficients were collected from the literature for comparison. Ruthven and Reyes [53] performed zero-length column (ZLC) experiments with SAPO-34 at 50 °C, and obtained an effective diffusion coefficient of 1.5×10^{-13} m^2/s and a diffusional activation energy of 19.60 kJ/mol for ethylene, and an effective diffusion coefficient of 9×10^{-14} m^2/s and a diffusional activation energy of 23.40 kJ/mol for propylene. The SAPO-34 zeolites were also investigated by Chen et al. [41], and they derived an effective diffusion coefficient of 1.2×10^{-13} m^2/s and a diffusional activation energy of 25.30 kJ/mol at 30 °C for methanol by use of a tapered element oscillating microbalance (TEOM). Nevertheless, the effective diffusion coefficients measured in our work agree well with the limited experimental data in the literatures. Fig. 7(B) shows the adsorption isotherms for methanol, ethylene, propylene and *iso*-butylene in SAPO-34 zeolites at 40 °C. The saturated adsorption capacity q^{sat} increases in the following order: *iso*-butylene < ethylene < propylene < methanol, which is in accordance with that for Si-CHA measured by Hedin et al. [42] and for SAPO-34 measured by Chen et al. [41], both using the

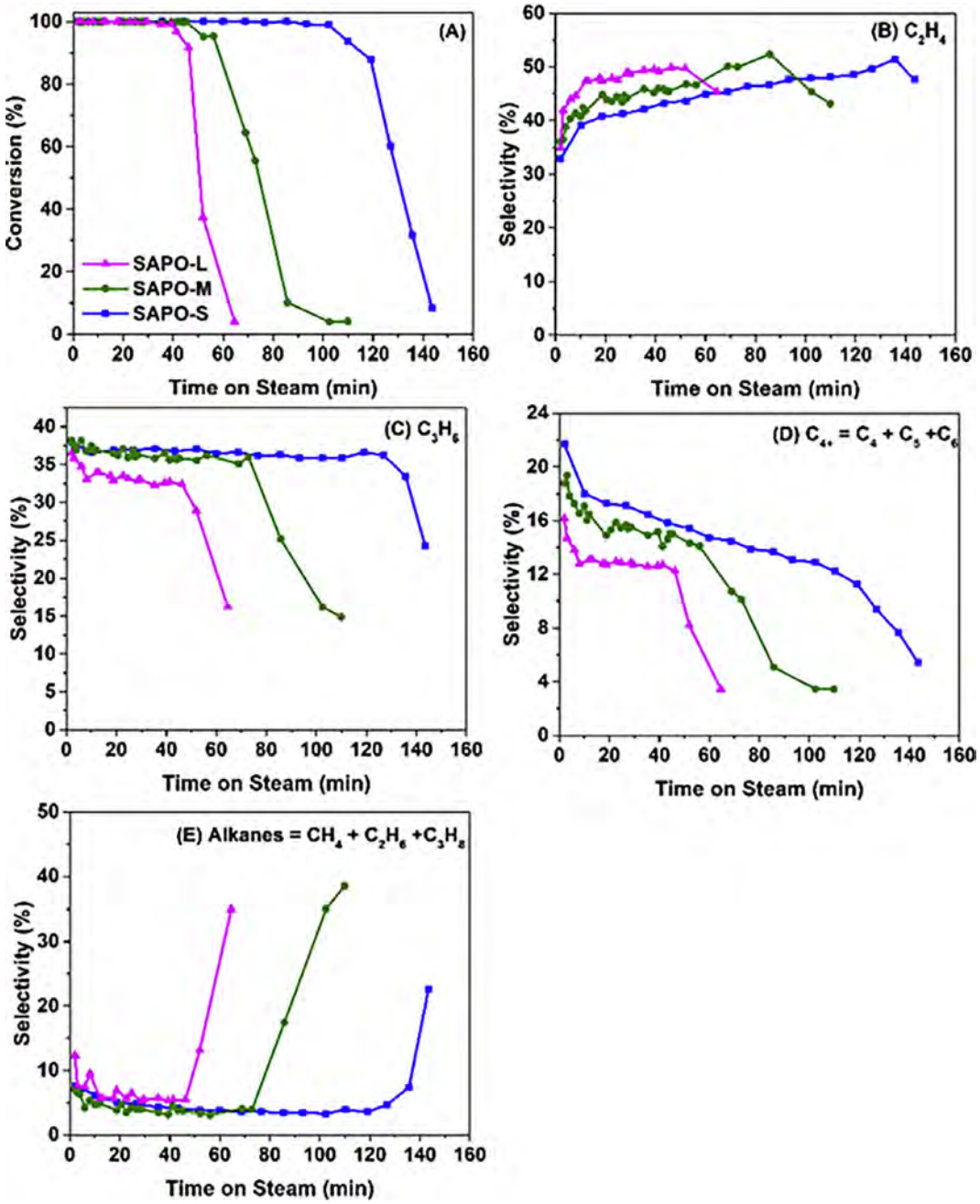

Fig. 5. (A) Methanol conversion, (B)–(E) products distribution as a function of time on steam in MTO reaction over SAPO-34 zeolites with different crystal size (C_{4+} lumps the products of C_4, C_5 and C_{6+}, alkanes lumps the products of methane, ethane and propane). Experimental conditions: T = 450 °C, WHSV = 5 $g_{MeOH} \cdot g_{zeo.}^{-1} \cdot h^{-1}$, partial pressure of methanol of 0.28 bar.

gravimetrical method. Table 1 lists the Langmuir adsorption parameters and the heat of adsorption of guest molecules measured in this work.

The deactivation of SAPO-34 zeolites in MTO process may be caused by the pore blocking and/or acid sites coverage due to coke deposition, which can be discriminated by an analysis of relative changes in the volumes of coke compounds formed and the changes in the pore volumes of the zeolites [54–56]. When coke compounds only cover the acid sites, the V_c/V_{na} ratio should be around 1. If coke deposition leads to not only acid sites coverage but also a pore blocking, it is expected V_c/V_{na} is smaller than 1. As shown in Fig. 8(A), V_c is determined by TGA, which is the weight of coke divided by the estimated density of coke compounds from [57], the detailed results could refer to Table S1. V_{na} is determined by N_2 physisorption, which is the volume of fresh SAPO-34 zeolites minus that of spent SAPO-34 zeolites with different quantity of coke. As can be seen in Fig. 8(A), the derived V_c/V_{na} ratio is smaller than 1, suggesting that the micropore blocking due to coke deposition is the main reason for deactivation of SAPO-34 zeolites in MTO process. V_c/V_{na} ratio keeps decreasing with time on stream, illustrating that the degree of pore blocking becomes more and more severe in the reaction process. Since the pore blocking mechanism with acid sites coverage is the predominant reason for deactivation, both the diffusion coefficient and diffusion pathway are expected to change. Therefore, as shown in Fig. 8(B) and Eq. (9), it is necessary to obtain the change of diffusion pathway with coke in order to quantify the change of diffusion coefficients with coke deposition. However, it is hard to characterize the diffusion pathway by experiments. Combining the reaction kinetics with diffusion, as depicted in Section 4.4, can provide the possible approach to study the effect of dynamic change of diffusion

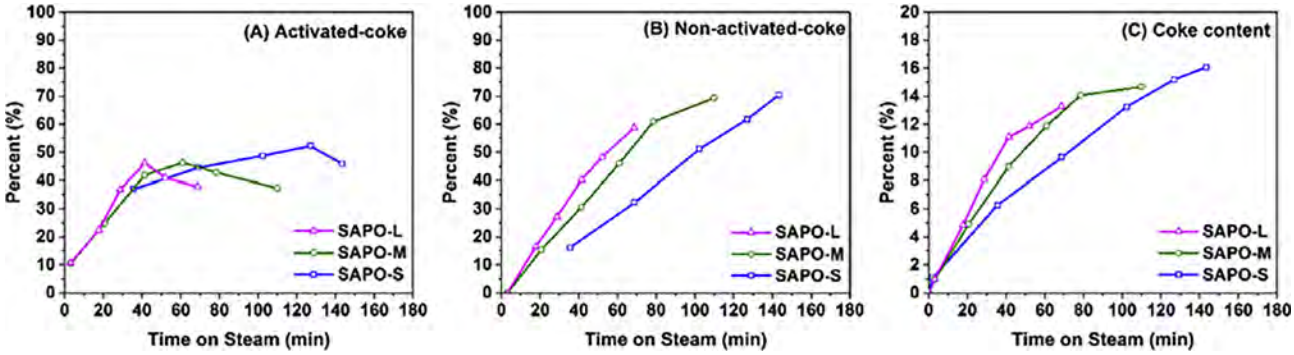

Fig. 6. The evolution of coke with time on steam: (A) activated-coke, (B) non-activated coke and (C) quantity of coke compounds over SAPO-34 zeolite with different crystal size. Experimental conditions: T = 450 °C, WHSV = 5 $g_{MeOH} \cdot g_{zeo.}^{-1} \cdot h^{-1}$, partial pressure of methanol of 0.28 bar.

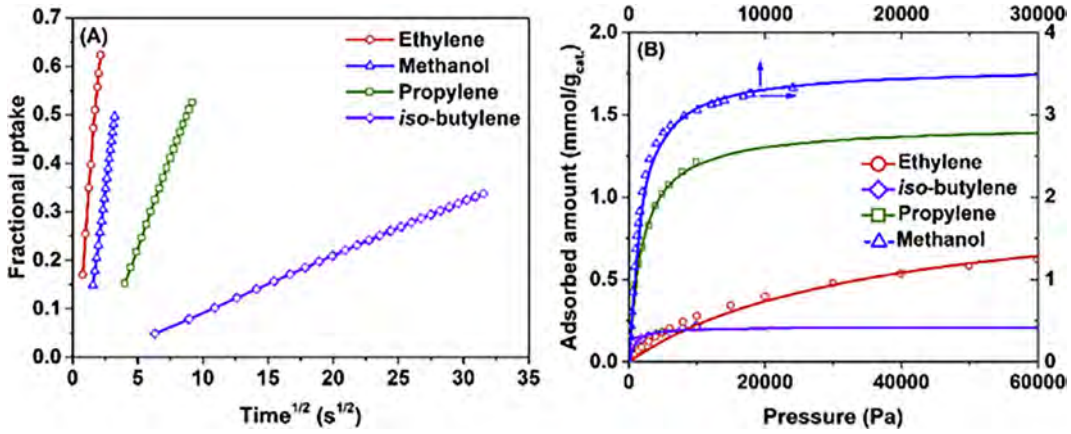

Fig. 7. (A) Uptake rates and (B) adsorption isotherms for methanol, ethylene, propylene and *iso*-butylene in the SAPO-34 zeolites at 40 °C, respectively. Solid lines represent Fick's second law fits in (A) and Langmuir fits in (B).

Table 1
The effective diffusion coefficient, diffusional activation energy, Langmuir adsorption parameters and the heat of adsorption for methanol, ethylene, propylene, *iso*-butylene and methane over SAPO-34 zeolites from experimental measurements and literatures.

guest molecule	D (m^2/s)	E_a (kJ/mol)	q^{sat} (mmol/$g_{zeo.}$)	b (Pa^{-1})	-ΔH_{ads} (kJ/mol)
Methanol	9.61×10^{-14}	25.26 [41]	3.58	1.24×10^{-3}	28.43 [41]
Ethylene	2.46×10^{-13}	19.60 [53]	0.87	3.94×10^{-5}	23.40
Propylene	1.18×10^{-14}	24.87 [53]	1.25	6.69×10^{-4}	25.16 [41]
iso-butylene	8.74×10^{-17}	42.40	0.23	8.31×10^{-4}	45.60 [59]
Methane [40,60]	1.10×10^{-11}	13.59	2.70	1.50×10^{-6}	16.00

The value with citation was collected from corresponding literature.

on MTO reaction. The effective diffusion coefficient in presence of different coke species can be estimated by Eq. (10). As found in [58], a certain quantity of molecular loading inside cage of CHA type zeolites could promote the diffusion coefficient of guest molecules. Analogously, the formation of activated coke inside cage of SAPO-34 zeolites, in particular, at the initial stage of MTO reaction, may enhance the diffusion coefficients of guest molecules. Meanwhile, the formation of non-activated coke would hinder the diffusion of guest molecules [5]. Table S1 lists the effect of coke deposition on the effective diffusion coefficients of reactant and main product molecules, which can be related to the quantity of activated and non-activated coke deposited in SAPO-34 zeolites by

$$D_i^{coke} = \exp(-A_i q_A) \cdot \exp(-B_i q_N) \quad (10)$$

where A_i and B_i ($kg_{zeo.}$/kg) are, respectively, the dimensionless quantity of activated an non-activated coke deposited in SAPO-34 zeolites, q_A and q_B are the mass loading quantity of activated and non-activated coke inside catalyst (kg/$kg_{zeo.}$).

Furthermore, the impact of coke amount on the adsorption isotherms are shown in Fig. 9. As can be seen from Fig. 9, the adsorption capacity of propane decreases significantly with the increasing quantity of coke, which is in accordance with the strong decrease of the accessible acid sites [10,11]. It is interesting to note that even with a rapid yet substantial decrease of the adsorption capacity and accessible Brønsted acid sites, SAPO-34 zeolites still exhibit a good performance in converting methanol, which may be due to the increase of activated coke as shown in Fig. 6. Based on the analysis of Fig. 9(B), a quantitative relation between adsorption capacity and the quantity of coke is established

$$q_i^{sat,coke} = q_i^{sat}\left(\frac{Coke_{max} - Coke}{Coke_{max}}\right)^2 \quad (11)$$

where $Coke_{max}$ is the maximum of coke content in SAPO-34 zeolites (wt %), and Coke is the coke content in SAPO-34 zeolites at different time on stream (wt%).

4.4. Simulation results

Based on the dual-cycle mechanism for MTO reaction (as shown in Fig. 3), the ethylene, propylene, C_{4+} and alkanes can be formed via the olefins-base cycle [31] while the main product molecules including

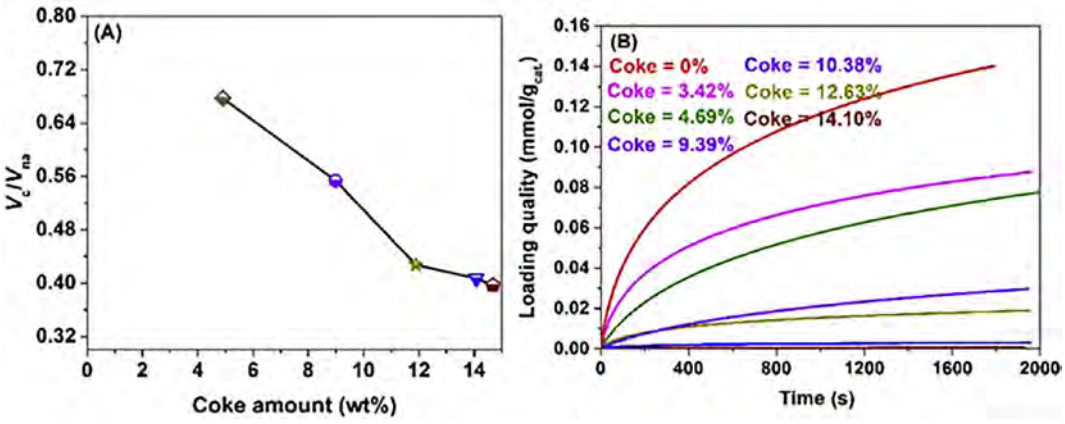

Fig. 8. (A) V_c/V_{na} of the catalyst with different coke amount and (B) propane uptake from 0 to 9 mbar at 40 °C on SAPO-34 zeolites with different coke amount.

ethylene and propylene can also be formed from the aromatic-base cycle, and the formation rate of ethylene is higher than that of propylene in reaction network (Table S1) [6]. The detailed reaction network and corresponding kinetic rate constants are listed in Table S1.

Fig. 10 shows the good agreement between the experimental and simulated results of methanol conversion and product selectivity for SAPO-34 zeolites with different crystal size. For smaller crystal size, higher selectivity of propylene and C_{4+} and lower selectivity of ethylene and alkanes at initial stage can be observed. Shortening the diffusion pathway and residence time of product molecules inside SAPO-34 zeolites suppresses the aromatization from preliminary olefin products. With relative low quantity of aromatic components in smaller crystals (Fig. 11) at initial stage, the formation of ethylene via aromatic-based cycle and formation of alkanes by hydrogen transfer reaction are also limited. As can be seen from Fig. 10, from initial stage until deactivation stage, the model can predict the changes of methanol conversion and product selectivity with good accuracy. It should be stressed that in current model no empirical expression to account for the deactivation of SAPO-34 zeolites in reaction kinetics is required, and the deactivation is a natural result of the formation of non-activated coke. To gain more insight, the simulation results of relative amount of acid sites, quantity of activated-coke and non-activated coke, and total quantity of coke deposited in SAPO-34 zeolites are shown in Fig. 11. With the evolution of time on steam, the amount of acid sites decreases exponentially, which matches well with the results on accessible acid sites measured by ^{1}H MAS NMR [10]. At the initial and steady reaction stage, the consumption rate of acid sites is relative slow for smaller crystal size, due to the shorter residence time of product molecules. After complete deactivation of catalyst, there are about 20% percent of inaccessible free acid sites surrounding by aromatic compounds. The amount of retained acid sites increase in the following order: SAPO-S < SAPO-M < SAPO-L, verifying that downsizing the SAPO-34 zeolite crystal could enhance the utilization and accessibility of acid sites. It is further noticed that the quantity of retained activated-coke is also lower for smaller crystal size. Since the activated coke is the intermediate product in MTO reaction, the maximum of quantity of activated-coke could be observed with time on steam, as shown in Fig. 11(B). Increasing accessibility of acid sites and quantity of activated-coke not only improves the catalytic lifetime but also promotes the maximum yield of poly-cyclic aromatic compounds. As shown in Fig. 11(C), after complete catalyst deactivation, the quantity of entrapped non-activated coke is increased for smaller crystal size. The total quantity of coke also increased in SAPO-34 zeolites with smaller crystal size after complete deactivation. Notably, the simulation results based on our reaction and diffusion model are consistent with the observation in experiments. On the basis of above discussion, the developed reaction and diffusion model in this work could reasonably capture the shift of selectivity of product molecules with the evolution of time on stream, and the effect of crystal size on the catalyst lifetime. In addition to that, the model can reveal the evolution of the amount of free acid sites, the quantity of activated coke and non-activated coke, and coke content inside SAPO-34 zeolites during the reaction, which is difficult to measure in experiments [11,50].

The direct and *in-situ* monitoring of the dynamic change of diffusion under reaction conditions remains a significant challenge, especially for catalyst with coke deposition [61]. Under *in-situ* reaction conditions, Fig. 12 shows the effect of coke deposition on the effective diffusion coefficients for various guest molecules. At the initial stage, the predominant aromatic compounds formed are the monocyclic and bicyclic aromatics, which may only occupy the acid sites but not block the

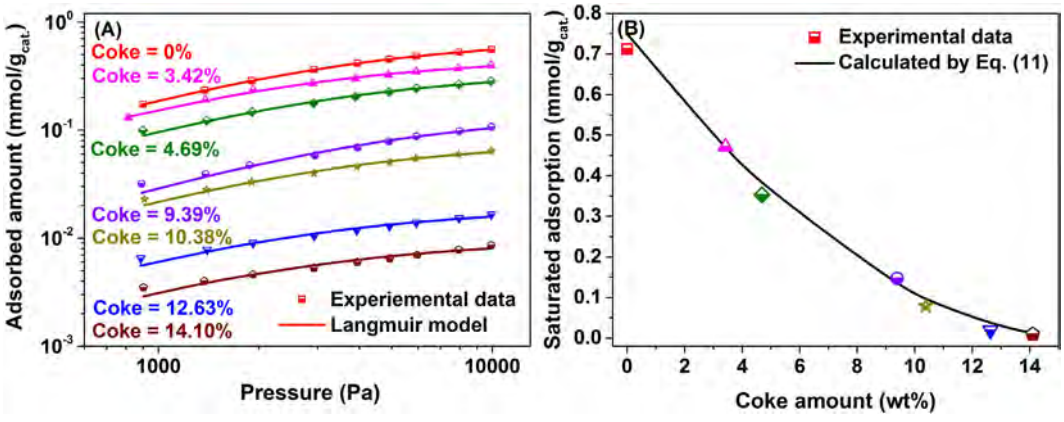

Fig. 9. (A) Adsorption isotherms of propane and (B) saturated adsorption capacity of propane on SAPO-34 zeolites with different amount of coke compounds at 40 °C.

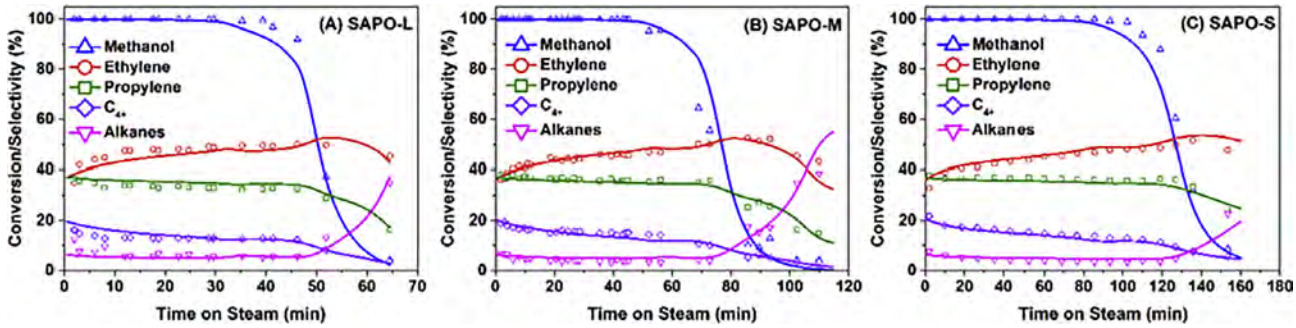

Fig. 10. Methanol conversion and products distribution as a function of time on steam in MTO reaction over SAPO-34 zeolites with different crystal size. Solid lines represent the simulation results of the reaction and diffusion model and discrete points represent the experimental data. Simulated conditions: $T = 450\ ^{\circ}C$, WHSV = $5\ g_{MeOH} \cdot g_{zeo.}^{-1} \cdot h^{-1}$, partial pressure of methanol of 0.28 bar.

micropores. Thus the effective diffusion coefficients for various guest molecules almost maintain unaffected by the low-cyclic aromatics. As the reaction proceeds, the tricyclic and polycyclic aromatics gradually deposit in the SAPO-34 zeolites, which could cause the pore blockage. As can be seen in Fig. 12, after the initial stage, a decrease of the effective diffusion coefficients of the reactant and products could be observed, but the degree of decrease varies extend for different guest molecules. This means the effect of pore blocking on diffusion coefficients depends on the molecule sizes. As for smaller molecules, the diffusion coefficient of methane just slightly slows down and methanol decreases about two orders of magnitude in presence of coke deposition. But for the larger molecules such as ethylene, propylene and C_{4+}, the diffusion coefficients show significant decrease. And at the complete deactivation stage, the effective diffusion coefficients drop by about four orders of magnitude. As shown in Fig. 10(C), due to the significant diffusion hindrance by coke deposition, part of product molecules are entrapped inside SAPO-34 zeolites leading to sustained increasement of non-activated as speculated in [5]. The diffusion coefficient of ethylene is still higher than that of propylene and C_{4+}, as can be seen from Fig. 10 at the complete deactivation stage, thus the selectivity to ethylene still increases, but the selectivity to propylene and C_{4+} begins to decrease.

Based on the experimental observation and simulation results, we propose the pathway for reaction and diffusion in MTO process over SAPO-34 zeolites, as represented in Fig. 13. As the product molecules form, some molecules will diffuse outwards the zeolite crystal and react with other molecules to form activated coke and non-activated coke. Due to different residence time of product molecules inside zeolites with different crystal size, the formation rate of the activated and non-activated coke can vary. Formation of activated coke will enhance the selectivity to ethylene, but formation of non-activated coke will cause the pore blocking, which will affect the diffusion coefficient of guest

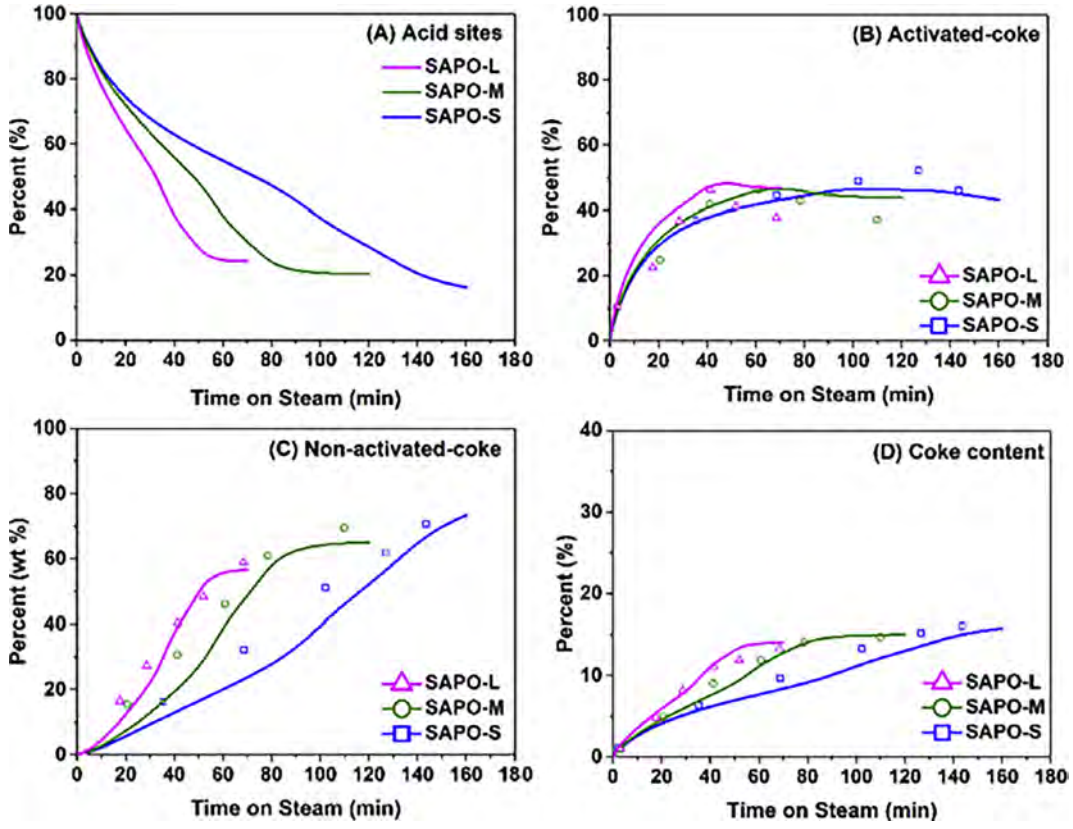

Fig. 11. The relative quantity of (A) acid sites, (B) activated-coke, (C) non-activated coke and (D) quantity of coke compounds as a function of time on stream in MTO reaction over SAPO-34 zeolites with different crystal size. Solid lines represent the simulation results of the reaction and diffusion model and discrete points represent the experimental data. Simulated conditions: $T = 450\ ^{\circ}C$, WHSV = $5\ g_{MeOH} \cdot g_{zeo.}^{-1} \cdot h^{-1}$, partial pressure of methanol of 0.28 bar.

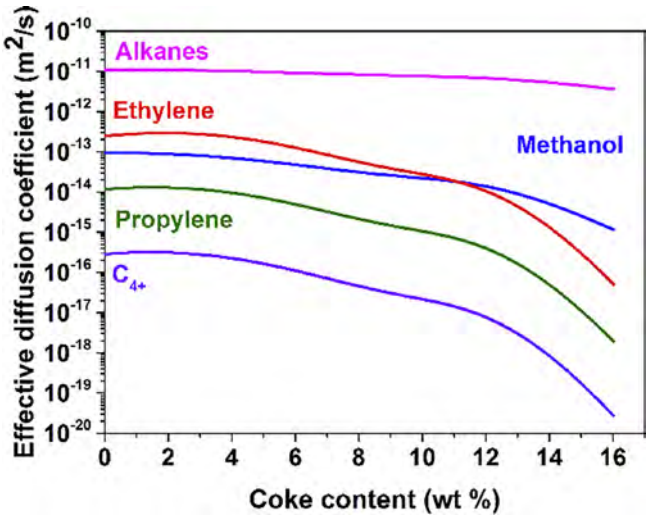

Fig. 12. The effective diffusion coefficients for methanol, ethylene, propylene, C_{4+} and alkanes as a function of coke content over SAPO-34 zeolites under *in-situ* reaction conditions, obtained from the simulation results of the reaction and diffusion model.

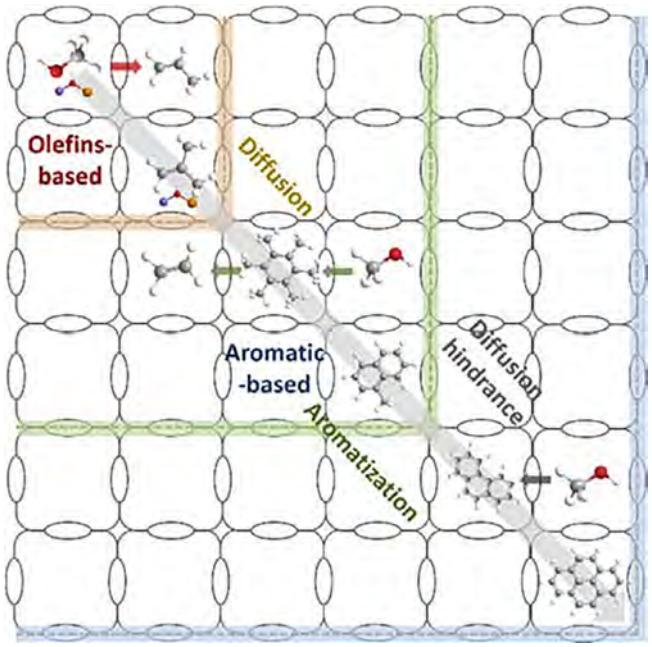

Fig. 13. Possible reaction and diffusion pathway inside SAPO-34 zeolite for MTO reaction.

molecules to various extend dependent upon the molecule size and crystal size.

5. Conclusion

A modeling approach was developed in which the reaction and diffusion in MTO process over SAPO-34 zeolites was taken into account. In this model, the dual-cycle mechanism for MTO reaction and the Maxwell-Stefan theory for diffusion was considered. The effective diffusion coefficients of guest molecules and adsorption isotherms over SAPO-34 zeolites were measured by IGA technique. The modeling results of MTO reaction over SAPO-34 zeolites with different crystal size was compared with experimental data in a fixed bed reactor, which shows a good agreement in terms of catalyst lifetime and a shift in product molecules selectivity. The evolution of acid sites, activated and non-activated coke components were captured by the model, which is normally hard to be directly measured in *in-situ* experiments. It is found that pore blocking is the dominant reason for catalyst deactivation in MTO reaction, and it affects the diffusion coefficient of guest molecules to various extend dependent upon the molecule size and crystal size. It should be stressed that in this model no empirical expression to account for the deactivation of SAPO-34 zeolites in reaction kinetics was required, and the deactivation is a natural result of the formation of non-activated coke. Also by introducing the activated coke, the auto-catalytic process in MTO reaction can be implicitly included. Though this work is the first step to model the influence of diffusion on MTO reaction, the aforementioned features of this model make it a potential tool for rational catalyst design, particularly, in terms of optimization of acid properties and pore structure.

Acknowledgements

This work is supported by the National Key Research and Development Program of China (Grant No. 2018YFB0604904).

Appendix A. Supplementary information

Supplementary data associated with this article can be found, in the online version, at https://doi.org/10.1016/j.cej.2018.08.054.

References

[1] U. Olsbye, S. Svelle, M. Bjørgen, P. Beato, T.V.W. Janssens, F. Joensen, S. Bordiga, K.P. Lillerud, Conversion of methanol to hydrocarbons: how zeolite cavity and pore size controls product selectivity, Angew. Chem. Int. Ed. 51 (2012) 5810–5831.
[2] P. Tian, Y. Wei, M. Ye, Z. Liu, Methanol to olefins (MTO): from fundamentals to commercialization, ACS Catal. 5 (2015) 1922–1938.
[3] M. Ye, H. Li, Y. Zhao, T. Zhang, Z. Liu, Chapter five – MTO processes development: the key of mesoscale studies, in: G.B. Marin, J. Li (Eds.), Advances in Chemical Engineering, Academic Press, 2015, pp. 279–335.
[4] I.M. Dahl, S. Kolboe, On the reaction mechanism for hydrocarbon formation from methanol over SAPO- 34: 2. isotopic labeling studies of the co-reaction of propene and methanol, J. Catal. 161 (1996) 304–309.
[5] B.P.C. Hereijgers, F. Bleken, M.H. Nilsen, S. Svelle, K.-P. Lillerud, M. Bjørgen, B.M. Weckhuysen, U. Olsbye, Product shape selectivity dominates the Methanol-to-Olefins (MTO) reaction over H-SAPO-34 catalysts, J. Catal. 264 (2009) 77–87.
[6] S. Wang, Y. Chen, Z. Wei, Z. Qin, H. Ma, M. Dong, J. Li, W. Fan, J. Wang, Polymethylbenzene or alkene cycle? Theoretical study on their contribution to the process of methanol to olefins over H-ZSM-5 zeolite, J. Phys. Chem. C 119 (2015) 28482–28498.
[7] J.S. Martínez-Espín, K. De Wispelaere, T.V.W. Janssens, S. Svelle, K.P. Lillerud, P. Beato, V. Van Speybroeck, U. Olsbye, Hydrogen transfer versus methylation: on the genesis of aromatics formation in the methanol-to-hydrocarbons reaction over H-ZSM-5, ACS Catal. 7 (2017) 5773–5780.
[8] M. Bjørgen, U. Olsbye, S. Kolboe, Coke precursor formation and zeolite deactivation: mechanistic insights from hexamethylbenzene conversion, J. Catal. 215 (2003) 30–44.
[9] J.F. Haw, D.M. Marcus, Well-defined (supra)molecular structures in zeolite methanol-to-olefin catalysis, Top. Catal. 34 (2005) 41–48.
[10] W. Dai, M. Scheibe, L. Li, N. Guan, M. Hunger, Effect of the methanol-to-olefin conversion on the PFG NMR self-diffusivities of ethane and ethene in large-crystalline SAPO-34, J. Phys. Chem. C 116 (2012) 2469–2476.
[11] W. Dai, G. Wu, L. Li, N. Guan, M. Hunger, Mechanisms of the deactivation of SAPO-34 materials with different crystal sizes applied as MTO catalysts, ACS Catal. 3 (2013) 588–596.
[12] J. Zhong, J. Han, Y. Wei, S. Xu, Y. He, Y. Zheng, M. Ye, X. Guo, C. Song, Z. Liu, Increasing the selectivity to ethylene in the MTO reaction by enhancing diffusion limitation in the shell layer of SAPO-34 catalyst, Chem. Commun. 54 (2018) 3146–3149.
[13] Y. Li, C. Zhang, C. Li, Z. Liu, W. Ge, Simulation of the effect of coke deposition on the diffusion of methane in zeolite ZSM-5, Chem. Eng. J. 320 (2017) 458–467.
[14] D. Chen, K. Moljord, A. Holmen, A methanol to olefins review: Diffusion, coke formation and deactivation on SAPO type catalysts, Microporous Mesoporous Mater. 164 (2012) 239–250.
[15] I.M. Dahl, R. Wendelbo, A. Andersen, D. Akporiaye, H. Mostad, T. Fuglerud, The effect of crystallite size on the activity and selectivity of the reaction of ethanol and 2-propanol over SAPO-34, Microporous Mesoporous Mater. 29 (1999) 159–171.
[16] N. Nishiyama, M. Kawaguchi, Y. Hirota, D. Van Vu, Y. Egashira, K. Ueyama, Size control of SAPO-34 crystals and their catalyst lifetime in the methanol-to-olefin reaction, Appl. Catal. A 362 (2009) 193–199.
[17] K.Y. Lee, H.-J. Chae, S.-Y. Jeong, G. Seo, Effect of crystallite size of SAPO-34 catalysts on their induction period and deactivation in methanol-to-olefin reactions,

Appl. Catal. A 369 (2009) 60–66.
[18] H.-G. Jang, H.-K. Min, J.K. Lee, S.B. Hong, G. Seo, SAPO-34 and ZSM-5 nanocrystals' size effects on their catalysis of methanol-to-olefin reactions, Appl. Catal. A 437–438 (2012) 120–130.
[19] G. Yang, Y. Wei, S. Xu, J. Chen, J. Li, Z. Liu, J. Yu, R. Xu, Nanosize-enhanced lifetime of SAPO-34 catalysts in methanol-to-olefin reactions, J. Phys. Chem. C 117 (2013) 8214–8222.
[20] D. Cai, Y. Ma, Y. Hou, Y. Cui, Z. Jia, C. Zhang, Y. Wang, F. Wei, Establishing a discrete Ising model for zeolite deactivation: inspiration from the game of Go, Catal. Sci. Technol. 7 (2017) 2440–2444.
[21] A.N.R. Bos, P.J.J. Tromp, H.N. Akse, Conversion of methanol to lower olefins. kinetic modeling, reactor simulation, and selection, Ind. Eng. Chem. Res. 34 (1995) 3808–3816.
[22] D. Chen, A. Grønvold, K. Moljord, A. Holmen, Methanol conversion to light olefins over SAPO-34: reaction network and deactivation kinetics, Ind. Eng. Chem. Res. 46 (2007) 4116–4123.
[23] A.G. Gayubo, A.T. Aguayo, A. Alonso, J. Bilbao, Kinetic Modeling of the methanol-to-olefins process on a silicoaluminophosphate (SAPO-18) catalyst by considering deactivation and the formation of individual olefins, Ind. Eng. Chem. Res. 46 (2007) 1981–1989.
[24] X. Yuan, H. Li, M. Ye, Z. Liu, Comparative study of MTO kinetics over SAPO-34 catalyst in fixed and fluidized bed reactors, Chem. Eng. J. 329 (2017) 35–44.
[25] L. Ying, X. Yuan, M. Ye, Y. Cheng, X. Li, Z. Liu, A seven lumped kinetic model for industrial catalyst in DMTO process, Chem. Eng. Res. Des. 100 (2015) 179–191.
[26] W. Wu, W. Guo, W. Xiao, M. Luo, Dominant reaction pathway for methanol conversion to propene over high silicon H-ZSM-5, Chem. Eng. Sci. 66 (2011) 4722–4732.
[27] T.-Y. Park, G.F. Froment, Kinetic modeling of the methanol to olefins process. 1. model formulation, Ind. Eng. Chem. Res. 40 (2001) 4172–4186.
[28] T.-Y. Park, G.F. Froment, Kinetic modeling of the methanol to olefins process. 2. Experimental results, model discrimination, and parameter estimation, Ind. Eng. Chem. Res. 40 (2001) 4187–4196.
[29] S.M. Alwahabi, G.F. Froment, Single event kinetic modeling of the methanol-to-olefins process on SAPO-34, Ind. Eng. Chem. Res. 43 (2004) 5098–5111.
[30] P. Kumar, J.W. Thybaut, S. Svelle, U. Olsbye, G.B. Marin, Single-event microkinetics for methanol to olefins on H-ZSM-5, Ind. Eng. Chem. Res. 52 (2013) 1491–1507.
[31] P. Kumar, J.W. Thybaut, S. Teketel, S. Svelle, P. Beato, U. Olsbye, G.B. Marin, Single-event microkinetics (SEMK) for methanol to hydrocarbons (MTH) on H-ZSM-23, Catal. Today 215 (2013) 224–232.
[32] R. Krishna, J.A. Wesselingh, The Maxwell-Stefan approach to mass transfer, Chem. Eng. Sci. 52 (1997) 861–911.
[33] H. Li, M. Ye, Z. Liu, A multi-region model for reaction-diffusion process within a porous catalyst pellet, Chem. Eng. Sci. 147 (2016) 1–12.
[34] P.J. Donaubauer, O. Hinrichsen, A monte-carlo-based sensitivity analysis of multicomponent diffusion in porous catalysts, Chem. Eng. Sci. 185 (2018) 282–291.
[35] J. Keil Frerich, R. Krishna, M.-O. Coppens, Modeling of diffusion in zeolites, Rev. Chem. Eng. 16 (2000) 71.
[36] B. Smit, T.L.M. Maesen, Molecular simulations of zeolites: adsorption, diffusion, and shape selectivity, Chem. Rev. 108 (2008) 4125–4184.
[37] A.L. Myers, J.M. Prausnitz, Thermodynamics of mixed-gas adsorption, AlChE J. 11 (1965) 121–127.
[38] R. Krishna, Problems and pitfalls in the use of the fick formulation for intraparticle diffusion, Chem. Eng. Sci. 48 (1993) 845–861.
[39] O. Levenspiel, Chemical Reaction Engineering, Third ed., Wiley, New York, 1999.
[40] S. Li, J.L. Falconer, R.D. Noble, SAPO-34 membranes for CO2/CH4 separation, J. Membr. Sci. 241 (2004) 121–135.
[41] D. Chen, H.P. Rebo, K. Moljord, A. Holmen, Methanol conversion to light olefins over SAPO-34. Sorption, diffusion, and catalytic reactions, Ind. Eng. Chem. Res. 38 (1999) 4241.
[42] N. Hedin, G.J. DeMartin, W.J. Roth, K.G. Strohmaier, S.C. Reyes, PFG NMR self-diffusion of small hydrocarbons in high silica DDR CHA and LTA structures, Microporous Mesoporous Mater. 109 (2008) 327–334.
[43] G. C.W., Numerical Initial Value Problems in Ordinary Differential Equations. Prentice-Hall, Englewood Cliffs, New Jersey1971.
[44] L. Ying, M. Ye, Y.W. Cheng, X. Li, Characteristics of coke deposition over a SAPO-34 catalyst in the methanol-to-olefins reaction, Pet. Sci. Technol. 33 (2015) 984–991.
[45] K. Hemelsoet, A. Nollet, V. Van Speybroeck, M. Waroquier, Theoretical simulations elucidate the role of naphthalenic species during methanol conversion within H-SAPO-34, Chem. Eur. J. 17 (2011) 9083–9093.
[46] W. Dai, C. Wang, M. Dyballa, G. Wu, N. Guan, L. Li, Z. Xie, M. Hunger, Understanding the early stages of the methanol-to-olefin conversion on H-SAPO-34, ACS Catal. 5 (2015) 317–326.
[47] H. Schulz, M. Wei, Pools and constraints in methanol conversion to olefins and fuels on zeolite HZSM5, Top. Catal. 57 (2014) 683–692.
[48] X. Yuan, H. Li, M. Ye, Z. Liu, Kinetic Modeling of Methanol to Olefins Process over SAPO-34.
[49] M. Yang, P. Tian, C. Wang, Y. Yuan, Y. Yang, S. Xu, Y. He, Z. Liu, A top-down approach to prepare silicoaluminophosphate molecular sieve nanocrystals with improved catalytic activity, Chem. Commun. 50 (2014) 1845–1847.
[50] M. Guisnet, "Coke" molecules trapped in the micropores of zeolites as active species in hydrocarbon transformations, J. Mol. Catal. A Chem. 182–183 (2002) 367–382.
[51] C. Wang, M. Yang, P. Tian, S. Xu, Y. Yang, D. Wang, Y. Yuan, Z. Liu, Dual template-directed synthesis of SAPO-34 nanosheet assemblies with improved stability in the methanol to olefins reaction, J. Mater. Chem. A 3 (2015) 5608–5616.
[52] J. Kärger, D.M. Ruthven, D.N. Theodorou, Diffusion in Nanoporous Materials, Wiley-VCH, Weinheim, 2012.
[53] D.M. Ruthven, S.C. Reyes, Adsorptive separation of light olefins from paraffins, Microporous Mesoporous Mater. 104 (2007) 59–66.
[54] X. Feng, X. Duan, G. Qian, X. Zhou, D. Chen, W. Yuan, Au nanoparticles deposited on the external surfaces of TS-1: enhanced stability and activity for direct propylene epoxidation with H2 and O2, Appl. Catal. B 150–151 (2014) 396–401.
[55] J.L. Sotelo, M.A. Uguina, J.L. Valverde, D.P. Serrano, Deactivation of toluene alkylation with methanol over magnesium-modified ZSM-5 Shape selectivity changes induced by coke formation, Appl. Catal. A 114 (1994) 273–285.
[56] A. de Lucas, P. Canizares, A. Durán, A. Carrero, Coke formation, location, nature and regeneration on dealuminated HZSM-5 type zeolites, Appl. Catal. A 156 (1997) 299–317.
[57] D. Chen, H.P. Rebo, A. Holmen, Diffusion and deactivation during methanol conversion over SAPO-34: a percolation approach, Chem. Eng. Sci. 54 (1999) 3465.
[58] E. Beerdsen, D. Dubbeldam, B. Smit, Understanding diffusion in nanoporous materials, Phys. Rev. Lett. 96 (2006) 044501.
[59] J.F.M. Denayer, L.I. Devriese, S. Couck, J. Martens, R. Singh, P.A. Webley, G.V. Baron, Cage and window effects in the adsorption of n-alkanes on chabazite and SAPO-34, J. Phys. Chem. C 112 (2008) 16593–16599.
[60] S. Li, J.G. Martinek, J.L. Falconer, R.D. Noble, T.Q. Gardner, High-pressure CO2/CH4 separation using SAPO-34 membranes, Ind. Eng. Chem. Res. 44 (2005) 3220–3228.
[61] C. Chmelik, J. Kärger, In situ study on molecular diffusion phenomena in nanoporous catalytic solids, Chem. Soc. Rev. 39 (2010) 4864–4884.